Atmos. Meas. Tech. Discuss., https://doi.org/10.5194/amt-2017-321
Manuscript under review for journal Atmos. Meas. Tech.
Discussion started: 10 November 2017

Atmospheric Measurement Techniques Discussions

Alternative Strategy for Estimating Zenith Tropospheric Delay from Precise Point Positioning

Jareer Mohammed [*a,b], Terry Moore[a], Chris Hill[a], Richard M. Bingley[c]

[a]Nottingham Geospatial Institute, University of Nottingham, UK

[b]Civil Engineering Department, College of Engineering, University of Wasit, Iraq

[c]NERC British Isles continuous GNSS Facility (BIGF), University of Nottingham, UK

***Corresponding author: jareermohammed@uowasit.edu.iq**

Abstract: This study considered zenith total delay (ZTD) estimation from precise point positioning (PPP) based on GPS only (PPP GPS), GLONASS only (PPP GLO), and GPS+GLONASS (PPP GPS+GLO) using both a conventional strategy when applying a model for the hydrostatic component with an estimation of the wet component and an alternative strategy. The proposed alternative strategy is to estimate both the hydrostatic and the wet components of the tropospheric delay using different process noises with different mapping functions for both components in an extended Kalman filter (EKF). It was found that the receiver clock offsets and the estimated ambiguities would absorb some errors in the ZTD when using the conventional strategy. The RMS values of the differences between the double differenced (DD) GPS ZTD and the PPP ZTD, using the alternative strategy, were 6.5, 7.3, and 6.7 mm for PPP GPS, PPP GLO, and PPP GPS+GLO, respectively. The results were validated over one continuous week and then over one year. Validation was also performed through comparison with the IGS ZTD values, for 12 weeks, with an overall RMS of 5.9 mm and against IGS real-time products with an overall RMS of 8.1 mm. Furthermore, the alternative strategy also provided significant improvements in the 5 cm convergence time in the vertical coordinate component of the float ambiguity solutions to be on average, 51, 36 and 27 minutes for PPP GPS, PPP GLO and PPP GPS+GLO solutions respectively.

Keywords: precise point positioning (PPP), zenith total delay (ZTD), tropospheric models, real-time ZTD

Atmos. Meas. Tech. Discuss., https://doi.org/10.5194/amt-2017-321
Manuscript under review for journal Atmos. Meas. Tech.
Discussion started: 10 November 2017

Atmospheric Measurement Techniques Discussions

1. Introduction

One of the major sources of error affecting precise point positioning (PPP) (Zumberge et al., 1997) is the tropospheric delay of the GNSS signals. This is the delay of the signals as they propagate between the satellites and the user receiver, which is caused by the increased density of the troposphere. The delay is typically divided into wet and hydrostatic components. The total tropospheric delay is generally referred to as the zenith total delay (ZTD), which is derived from the individual slant delays using an appropriate mapping function. The zenith wet delay (ZWD) can be computed by simple subtraction of the zenith hydrostatic delay from the estimated ZTD. The hydrostatic delay is typically computed using atmospheric pressure data at the receiver, and the station's latitude and orthometric height (Saastamoinen, 1972). The atmospheric pressure can either be observed, obtained from numerical weather models or from climate datasets, such as the ERA-Interim products (Dee et al., 2011).

Many studies have been undertaken to improve the performance of ground-based GPS tropospheric delay estimation. Schueler et al. (2000) compared the ZTD estimated from their spatial interpolation of the tropospheric delay method with the IGS ZTD and found an agreement of 1.7 cm. Penna et al. (2001) compared the ZTD from the SBAS tropospheric model with that obtained from an analysis of one-year GPS carrier phase data analyzed and published by Dodson et al. (2000). They found that, for five stations in the United Kingdom, between 72% and 78% of the differences were <5 cm and between 96% and 99% were <10 cm. They also concluded that the RMS positioning errors in height component ranged from 4.0 to 4.7 cm, with maximum positioning errors ranging from 13.2 to 17.8 cm.

Leandro et al. (2006) presented and tested the UNB3m model as a modified version of the UNB3 model. They found that the predicted errors of the estimate of tropospheric delay from UNB3m had a mean value −0.5 cm and a standard deviation (STD) of 4.9 cm with respect to ray-tracing analysis. Furthermore, the treatment of the ZWD as a stochastic parameter, updated at every observation epoch in a Kalman filter, was found by Pany et al. (2007) to be a good tool with which to account for the high variability of the wet troposphere. Pace et al. (2010) presented a method for estimating ZTD residual fields using a ground-based GPS network. They modeled the zenith hydrostatic delay (ZHD) as an exponential function of latitude, whereas the ZWD was estimated every 5 minutes using a random walk stochastic model with a constraint of 20 mm/($\sqrt{h}$). They found that the ZTD residuals were of the order of 50–100 mm.

Atmos. Meas. Tech. Discuss., https://doi.org/10.5194/amt-2017-321
Manuscript under review for journal Atmos. Meas. Tech.
Discussion started: 10 November 2017

The results presented by Li et al. (2012), from 125 IGS stations during 2001-2005, summarized the magnitude of the bias and RMS of the differences between IGS ZTD and the estimated ZTD for the SBAS model (bias: 2.0 cm, RMS: 5.4 cm), UNB3 model (bias 2.0 cm, RMS: 5.4 cm), UNB3m model (bias 0.7 cm, RMS: 5.0 cm), and IGGtrop model (bias: −0.8 cm, RMS: 4.0 cm). Their results showed that the new IGGtrop model provided the smallest bias and RMS errors. However, the IGGtrop model is not available in the public domain and it still has a 4 cm RMS level of uncertainty.

Numerical weather models that rely on meteorological data are used widely to estimate the tropospheric delay. Yang et al. (2013) presented a new approach for estimating the slant tropospheric delay from high-resolution numerical weather modeling products. Their RMS of the differences between the tropospheric slant delay from the numerical weather model and the reverse computed tropospheric slant delay from PPP was 6 cm below 10°, < 3.5 cm above 15° and 2 cm above 30° elevation. Chen et al. (2014) mentioned that their model could predict the ZTD with average uncertainties of about 2 cm under normal atmospheric conditions. Böhm et al. (2014) presented a new blind tropospheric delay model (GPT2w) based on gridded values of water vapor pressure, a water vapor reduction factor, and weighted mean temperature. They also compared their model with three other blind models, referenced to the zenith total delay provided by IGS, as shown in Table 1.

Table 1 Summary of the numerical weather model comparison by Böhm et al. (2014)

Model	Mean bias of ZTD differences (cm)	Mean RMS of ZTD differences (cm)
SBAS	−2.50	4.55
ESA (Krueger et al., 2005)	0.83	3.82
GPT2 (Lagler et al., 2013)	−0.28	3.79
GPT2w	−0.02	3.61

All the tropospheric models used for providing the hydrostatic or wet components rely on measured data to predict the tropospheric delay. However, they cannot account for weather variation and thus, cannot provide highly accurate estimates of the tropospheric delay. Furthermore, none of the tropospheric models account for the diurnal variations of the troposphere. For example, they assume that pressure will be stable for a particular day of the year and that it will also be steady for

Atmos. Meas. Tech. Discuss., https://doi.org/10.5194/amt-2017-321
Manuscript under review for journal Atmos. Meas. Tech.
Discussion started: 10 November 2017

the same day from one year to the next. The assumption that the hydrostatic component will not change during the day is likely to be flawed. However, the accuracy of all the ZTD results obtained from the traditional models and the numerical models are within the range of centimeters, and those within the range of <1 cm have a standard deviation of about 5 cm (UNB3m bias, 0.7 cm; RMS, 5.0 cm compared to the zenith total delay provided by IGS).

The objective of this study was to assess the accuracy of tropospheric delay estimates that are achievable using different processing strategies. Most importantly, it considered a new alternative strategy for the estimation of high accuracy tropospheric delay estimation, from PPP, in static and real time situations.

2. Methodology

2.1. PPP Daily Solution Methodology

All the PPP solutions were processed using the POINT software, which was originally developed as part of the iNsight project (www.insight-gnss.org). The POINT software is programmed in C++ and its core is the EKF, as presented in Feng et al. (2008).

Undifferenced observations were used for each PPP daily solution using general observation equations for the code and phase as follows:

For the pseudorange (m):

$$P_F^i = \rho^i + c\delta_{r\_code} - c\delta^i + \frac{I^i}{f_F^2} + \frac{S^i}{f_F^3} + T^i + M_{PF}^i + Q_{PF}^i + bias_{P,F} - bias\,{}_{P,F}^{i} \quad (1)$$

For the carrier phase (m):

$$L_F^i = \rho^i + c\delta_{r\_phase} - c\delta^i - \frac{I^i}{f_F^2} - \frac{S^i}{f_F^3} + T^i + m_F^i + q_F^i + \lambda_F\left(N_F^i\right) \quad (2)$$

where i is the satellite index and F represents the index of the GNSS frequency. For GPS satellites, F = 1 (GPS L_1) and F = 2 (GPS L_2). For GLO satellites F = 1 (GLO L_1) and F = 2 (GLO L_2) with

$$f_{k\,L1} = f_{0L1} + k\Delta f_{L1} \quad (3)$$

$$f_{k\,L2} = f_{0L2} + k\Delta f_{L2} \quad (4)$$

Here, k represents the frequency channel: f_{0L1} = 1602 MHz for GLONASS L_1 band, Δf_{L1} = 562.5 kHz frequency separation between the GLONASS carriers in the L1 band, f_{0L2} = 1246 MHz for GLONASS L_2 band, and Δf_{L2} = 437.5 kHz frequency separation between the GLONASS carriers in

Atmos. Meas. Tech. Discuss., https://doi.org/10.5194/amt-2017-321
Manuscript under review for journal Atmos. Meas. Tech.
Discussion started: 10 November 2017

the L_2 band. In the above, ρ^i represents the geometric distance from the receiver to the satellite, $c\delta_{r-code}$ is the receiver clock offset for code, $c\delta_{r-phase}$ is the receiver clock offset for phase, $c\delta^i$ is the satellite clock offset,

I^i is the first-order ionospheric bias term, S^i is the second-order ionospheric bias term, f_F is the GNSS frequency, T^i is the tropospheric bias. M_F^i is the multipath error for pseudorange, m_F^i is the multipath error for carrier-phase, Q_F^i is the noise for the pseudorange, q_F^i is the noise for the carrier-phase. $bias_{P,F}$ is the receiver code bias for pseudorange, $bias_{P,F}^i$ is the satellite code bias for pseudorange, λ_F is the wavelength, N_F^i is the carrier phase ambiguity term.

For all the PPP daily solutions, a decoupled receiver clock (separate clocks for code and carrier) is applied for both GPS and GLO (Collins et al., 2010), and the ionosphere-free observable is used without applying any second-order ionospheric bias corrections. The ionospheric-free combinations for the code and phase observables follow the process described by Dach et al. (2007). The processing settings for the PPP solutions are summarized in Table 2.

Table 2 The processing parameters for PPP solution.

Products (precise satellite coordinates and satellite clock offsets)	Natural Resources Canada (NRCan), unless otherwise mentioned.
Antenna phase centre offsets and variations	ANTEX from IGS, (Kouba, 2009).
Solid Earth tides, ocean tidal loading	Applied
Satellite Phase wind-up	Wu et al. (1993).
Pole and nutation motions	IERS conventions 2004 (McCarthy and Petit, 2004)
Carrier phase ambiguities	Float solution.
Cycle slip detection	Liu (2011)
Troposphere	Using Saastamoinen model for the hydrostatic component and estimate the wet as a state, unless otherwise mentioned.
Troposphere mapping function	New Mapping function (Niell, 1996) because of its capability for providing separate wet and dry mapping functions.
Tropospheric gradient	Chen model (Meindl et al., 2004), and using the Chen mapping function (Chen and Herring, 1997) .
Differential Code Bias	CODE (Dach et al., 2007).

Atmos. Meas. Tech. Discuss., https://doi.org/10.5194/amt-2017-321
Manuscript under review for journal Atmos. Meas. Tech.
Discussion started: 10 November 2017

Atmospheric Measurement Techniques Discussions

Weighting function	No weighting functions are applied to the observations, except for the observations noise that is needed for the EKF, which is set to 2.0 m for the pseudorange measurements and to 0.01 m for the carrier phase measurements for both GPS and GLO.

2.2. Global DD GPS Daily Solutions Methodology

For the UK stations, the processing strategy for the global DD GPS daily solutions is summarized in Table 3. Approximately 150 continuous GNSS stations (CGNSS) in the British Isles, including 100+ that are part of the Ordnance Survey of Great Britain (OSGB) national network, were included in the processing along with some 200+ IGS stations.

Table 3 The processing parameters for double difference solutions.

Software	Bernese GNSS Software version 5.2 (Dach et al., 2007) (Dach et al., 2009). Based on LSQ approach
Products (precise satellite coordinates and satellite clock offsets)	C13 (CODE repro2/repro_2013) re-analyzed satellite orbit and earth orientation parameter products
Satellite and receiver antenna phase center offsets and variations	I08.ATX models for antenna phase center variations
Troposphere	a-priori modeling of troposphere effects using VMF1G and estimation using zenith path delay and gradient parameters.
Ionosphere	mitigation of the first- and higher-order (second- and third-order and ray bending) ionospheric effects
Solid earth tides, Ocean tidal loading, and Atmospheric tidal loading	Applied
Carrier phase ambiguities	Fixed ambiguity.

2.3. New Strategy for Estimating Tropospheric Delay

The new PPP processing strategy is to estimate both components of the troposphere (hydrostatic and wet) without relying solely on a tropospheric model for the hydrostatic component. The partial

Atmos. Meas. Tech. Discuss., https://doi.org/10.5194/amt-2017-321
Manuscript under review for journal Atmos. Meas. Tech.
Discussion started: 10 November 2017

derivative used in the design matrix is derived from the mapping function for the dry and wet components, respectively:

$$\frac{\partial d_{trop}}{\partial d_h} = m(\varepsilon)_h \qquad (5)$$

$$\frac{\partial d_{trop}}{\partial d_w} = m(\varepsilon)_w \qquad (6)$$

where $m(\varepsilon)_h$ and $m(\varepsilon)_w$ are the mapping functions for the hydrostatic component and the wet component respectively.

To allow the estimation process to properly reflect the characteristics of the two components of the troposphere, the process noise for the two components has to be chosen carefully. The hydrostatic component of the tropospheric delay is relatively stable and predictable, whereas the wet component is more variable and less predictable since it depends on the distribution of water vapour in the atmosphere. A higher process noise for the wet component allows the value to converge more quickly even if the initial value is not accurate, and it allows the value to change rapidly in response to real physical changes.

Since the wet and dry mapping functions and hence the partials used to estimate the components are similar, it is not expected that the estimation process will determine reliable values for these two components, but we expect that the sum of these two estimated components will reflect the ZTD accurately. Therefore, the process noise and the initial values had to be chosen quite carefully in order to provide a balanced, and optimal performance from the processing.

This tropospheric estimation strategy does not rely on the availability of meteorological data or models. The values for the random-walk process noise were chosen empirically as 1e-5 m/$\sqrt{sec}$ and 3e-5 m/$\sqrt{sec}$ for the hydrostatic and wet components, respectively. We treat the hydrostatic components as datum for the ZTD and the wet component will be the variation component of the ZTD. Thus, we will end up with a ZTD with a good consistency with the ZTD from the independent DD processing. Bear in mind that the validation will only be addressed by the ZTD components because at this stage we are not attempting to separately validate the two components.

3. Datasets for Comparing the Two Methods

For the purposes of this study, a data set focusing on the 100+ OSGB CGNSS stations that have daily RINEX observation data files archived as part of NERC British Isles continuous GNSS Facility

Atmos. Meas. Tech. Discuss., https://doi.org/10.5194/amt-2017-321
Manuscript under review for journal Atmos. Meas. Tech.
Discussion started: 10 November 2017

Atmospheric Measurement Techniques Discussions

(BIGF) and that were included in the global DD GPS daily solutions created by BIGF was chosen. The locations of the CGNSS stations are illustrated in Figure 1.

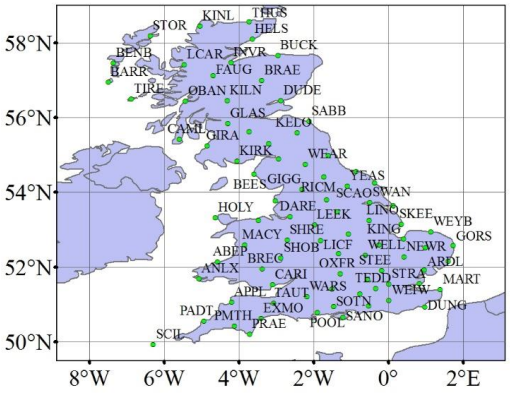

Fig. 1 The 100+ OSGB CGNSS stations included in BIGF that were used for the assessment of the new tropospheric strategy in this study

A 7-week period (detailed in Table 4) was used for the evaluation of the tropospheric delay using the different tropospheric models. Only those OSGB CGNSS stations that operated continuously for a specific GPS week with optimum 24-h observations recording each day and that were also present in the global DD daily solutions were included. This led to the availability of 56–85 OSGB CGNSS stations per week of the analysis, as detailed in Table 4.

Table 4 GPS week and the number of OSGB CGNSS stations considered in the analysis for each week.

Calendar days	GPS Week	No. of CGNSS Stations
12-18/1/2014	1775	56
19-25/1/2014	1776	85
26-01/2/2014	1777	79
02-09/2/2014	1778	74
09-15/3/2014	1783	74
16-22/3/2014	1784	76
23-29/3/2014	1785	79

Atmos. Meas. Tech. Discuss., https://doi.org/10.5194/amt-2017-321
Manuscript under review for journal Atmos. Meas. Tech.
Discussion started: 10 November 2017

3.1. Results using the Traditional Strategy

The 'traditional' PPP processing strategy uses a model for the hydrostatic component of the tropospheric delay and estimates a correction to an initial hydrostatic component, along with the other unknowns of the state vector. In this study, we have compared the effect of different models for the hydrostatic component, and to compute the initial wet component. The models used included the Saastamoinen model (Saastamoinen, 1973), UNB3m, which is a modified version of the University of New Brunswick's (UNB3) neutral atmosphere model (Leandro et al., 2006), GPT as presented by Boehm et al. (2007) and the SBAS model, which is one of the most commonly used tropospheric delay models (RTCA, 1996). The processing was performed as a static solution for every 24 h with an elevation cut-off angle of 10°.

To analyze the accuracy of the PPP solution, the RMS of the daily PPP difference from the DD GPS for all coordinate components were computed for the 7-week data set and for all situations using PPP GPS, PPP GLO, and PPP GPS+GLO. For the assessment of the accuracy of the determination of the tropospheric delay, the daily mean of the differences between the common epochs from the ZTD_{DD}, which is estimated every 1 hour, and ZTD_{PPP} ($ZTD_{PPP} - ZTD_{DD}$) was computed with the overall mean and overall RMS, as detailed in Table 5.

Table 5 RMS of the daily differences of coordinates and the differences of the ZTD

Model	Daily coordinate differences (RMS) (mm)			Tropospheric ZTD differences (mm)		
	E	N	U	Mean	STD	RMS
GPS						
UNB3m	3.7	3.1	7.5	45.8	9.9	46.8
GPT	3.7	3.2	7.1	75.7	7.7	76.1
Saastamoinen	3.6	3.1	7.6	58.3	17.3	60.8
SBAS	3.6	3.1	7.5	58.4	16.0	60.6
GLO						
UNB3m	3.7	4.9	11.5	44.5	11.1	45.9
GPT	3.7	4.9	12.7	75.0	8.7	75.5
Saastamoinen	3.7	4.9	10.7	57.0	18.9	60.1
SBAS	3.7	4.9	10.8	57.2	17.8	59.8
GPS+GLO						
UNB3m	3.6	3.9	8.3	44.9	10.5	46.1
GPT	3.7	3.9	8.6	74.5	8.0	74.9
Saastamoinen	3.8	4.0	7.8	57.5	17.8	60.1
SBAS	3.7	3.9	7.9	57.1	16.2	59.4

Atmos. Meas. Tech. Discuss., https://doi.org/10.5194/amt-2017-321
Manuscript under review for journal Atmos. Meas. Tech.
Discussion started: 10 November 2017

Table 5 shows the difference in the tropospheric models used for comparison with the ZTD from DD GPS. These results are consistent with the literature, e.g. Li et al. (2012) quote RMS differences of 5.4 cm, 5 cm and 4 cm for SBAS, UNB3m and IGGtrop respectively and Pace et al. (2010) quote residuals in the order 50-100 mm.

3.2. Results Using The New Strategy:

To test the reliability of the alternative strategy for tropospheric estimation, there is a need to conduct reasonable validations. All the following validations were conducted using OSGB or IGS stations in the GDD GPS solutions as a reference value for the comparison. In theory, the tropospheric ZTD from the GDD GPS represents a 'truth' value for the tropospheric delay. The reason is that it was computed using a network of stations capable of estimating tropospheric ZHD and ZWD between stations.

The validations were conducted using 7 consecutive days and regional validations at 56 OSGB stations using the PPP GPS, PPP GLO and the PPP GPS+GLO. Further, a long-term validation was also conducted using 22 OSGB stations for one year and using IGS stations.

4. Validation of the New strategy

4.1. Validation for One Continuous Week

To validate the new troposphelric strategy, it is important to test it over consecutive days to evaluate its ability to provide an accurate tropospheric ZTD. It is also interesting to use zero values for initializing the tropospheric ZHD and ZWD in PPP to test if the alternative tropospheric strategy with the used mapping functions is capable of providing an accurate tropospheric ZTD independent of the initial values. Therefore, this strategy was tested using 56 OSGB stations for seven consecutive days (one continuous solution not 7 x daily solutions) on DOY 12-18, 2014 (GPS week 1775) starting with zero initial values for tropospheric ZHD and ZWD. Figure 2 illustrates a sample of the ZTD estimates from one of the 56 stations for one continuous week. The degree of consistency between the estimated ZTD which is the sum of the estimated hydrostatic and wet components using the new strategy and the ZTD derived from DD GPS can be clearly seen and the results are summarized in Table 6. Bear in mind that this is a special example for one continuous week starting from zero initial values for the wet and the hydrostatic components using the new strategy.

Atmos. Meas. Tech. Discuss., https://doi.org/10.5194/amt-2017-321
Manuscript under review for journal Atmos. Meas. Tech.
Discussion started: 10 November 2017

Atmospheric Measurement Techniques Discussions

Table 6 RMS of the daily differences of coordinates and the differences of the ZTD for one continuous week using 56 stations.

Model	Daily difference (RMS) (mm)			Tropospheric difference (mm)		
	E	N	U	Mean	STD	RMS
The new strategy	GPS					
	1.9	1.6	14.1	-6.3	5.8	8.5

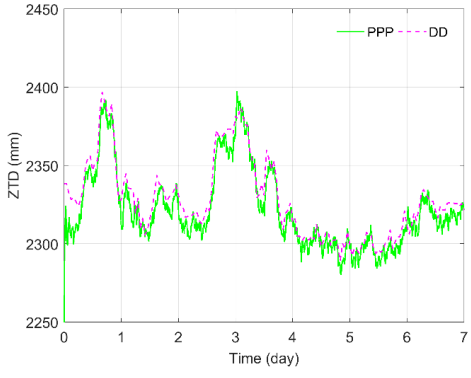

Fig. 2 Comparison between ZTD from DD GPS and PPP GPS for the ASAP station for one continuous week

It is evident from Figure 2 that the tropospheric ZTD using PPP GPS, which comes from the estimated tropospheric ZHD and ZWD, agrees strongly with the tropospheric ZTD from the GDD GPS. This alternative tropospheric strategy achieves this without using a model or any assumptions, nor any meteorological data. The selection of the initial nominal zero values for the hydrostatic and dry components was performed to establish whether the estimated values would converge to the correct ZTD value which in this case was taken as the ZTD value obtained from the DD GPS. In practice, as this will affect the convergence time, it is important to choose a suitable initial value, thus for future processing, more realistic initial values will be used. This approach also confirmed the suitability of the chosen mapping functions as well as the values selected for the process noise.

Atmos. Meas. Tech. Discuss., https://doi.org/10.5194/amt-2017-321
Manuscript under review for journal Atmos. Meas. Tech.
Discussion started: 10 November 2017

4.2. Regional Validation

To further evaluate the new processing strategy, it was important to process the same data set that had previously been processed when assessing the different tropospheric models (Table 4). Similar PPP configurations were adopted, except that the tropospheric delay was estimated using the new strategy with initial values of 2.1 m and 0.1 m for the dry and wet components, respectively. The PPP RMS of the daily difference is shown in Table 7 with a comparison of the tropospheric ZTD between the PPP situations and DD GPS.

Table 7 RMS of the daily difference of PPP solutions from the DD solutions for 7 weeks for all stations

Model	RMS Daily difference (mm)			Tropospheric difference (mm)		
	E	N	U	Mean	STD	RMS
The new strategy	GPS					
	3.6	3.1	8.3	-2.2	6.2	6.5
	GLO					
	3.7	4.8	7.3	-3.5	6.4	7.3
	GPS+GLO					
	3.9	3.9	7.1	-3.9	5.4	6.7

Again, this table can be compared with Table 5 (both Tables 5 & 7 are referring to the same datasets of Table 4, the only difference between them is the tropospheric strategy). It is clear from Table 7 that the ZTD derived from the estimated hydrostatic and the estimated wet components compares well with the values obtained from DD GPS. Thus, the new strategy provides a value of the ZTD without the need for models except for the mapping function models for the partial derivatives, assumptions for the hydrostatic or wet components, or even the meteorological data. Moreover, the rate at which ZTD estimates can be computed is a direct function of the observation rate. In our case, the 30 second observational epochs meant that ZTD values were available every 30 second.

4.3. Long-Term Validation of the New Strategy

The tropospheric delay varies daily and seasonally. Therefore, it is important to validate the new processing strategy for deriving the tropospheric delay over a longer term. To achieve this, data from day of year (DOY) 2 (02/01) to DOY 365 (31/12), of 2014, from six CGNSS stations was used for a complete one-year analysis, under the same PPP configuration, using the new strategy. For each

Atmos. Meas. Tech. Discuss., https://doi.org/10.5194/amt-2017-321
Manuscript under review for journal Atmos. Meas. Tech.
Discussion started: 10 November 2017

Atmospheric Measurement Techniques Discussions

station, the mean and the standard deviation of the differences between the ZTD estimates from PPP and DD were calculated. A summary of the results is shown in Figure 3.

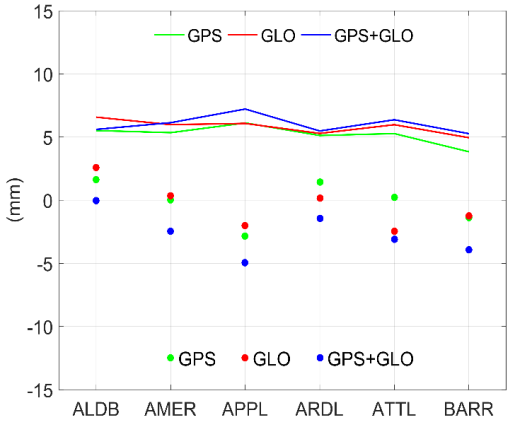

Fig. 3 One-year tropospheric mean differences (marker) from DD GPS and RMS differences (line) from DD GPS for six stations and all PPP cases.

The accuracy of the tropospheric delay estimations achievable for these stations can be seen in Figure 3. This illustrates that the new strategy may be used at any time of the year, irrespective of the weather conditions. Most importantly, the suitability of PPP GLO for the tropospheric delay estimation is clearly highlighted, since the performance of the PPP GLO situation appears no different from the PPP GPS situation. In addition, this gives the potential for PPP users to create two solutions for the same station, instead of one solution of PPP GPS or PPP GPS+GLO.

4.4. Global Validation using IGS Stations

For the validation of the new processing strategy over different locations, a number of IGS (Dow et al., 2009) stations were chosen, as illustrated in Figure 4, based on two conditions. Firstly, they had to be available for one continuous week to ensure continuity, and secondly, their solution had to be available from the IGS for the station coordinate estimation and, most importantly, for the final tropospheric solution. The chosen stations ranged between −68.57° and 74.7° latitude, −176.6° and 174.8° longitude, and −27.99 and 2228.3 m height. This degree of variation was selected to provide an indication of the effectiveness of adopting the new strategy for ZTD estimations.

Atmos. Meas. Tech. Discuss., https://doi.org/10.5194/amt-2017-321
Manuscript under review for journal Atmos. Meas. Tech.
Discussion started: 10 November 2017

Atmospheric Measurement Techniques Discussions

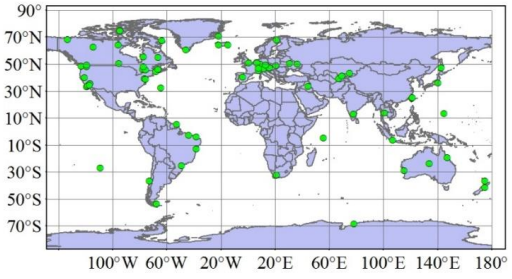

Fig. 4 IGS stations used for the assessment of the new tropospheric strategy in this study

To ensure that the method was tested for different weather activity throughout the year, we choose the first GPS week from each month. Table 8 shows the number of IGS stations available for each of the selected GPS weeks in 2014.

Table 8 GPS week and the number of IGS stations considered in the analysis of each week

Calendar days	GPS week	No. IGS stations
05-11/01/2014	1774	74
02-08/02/2014	1778	76
02-08/03/2014	1782	74
06-12/04/2014	1787	56
04-10/05/2014	1791	64
01-07/06/2014	1795	66
06-12/07/2014	1800	64
03-09/08/2014	1804	71
07-13/09/2014	1809	73
05-11/10/2014	1813	74
02-08/11/2014	1817	68
07-13/12/2014	1822	70

PPP daily solutions were compared with the IGS weekly solutions to overcome the variations of the IGS daily solutions. Two products (orbits, clocks) were used: the IGS final products and the NRCan products. For the ZTD comparison, two products are available from IGS: one is for near real time, which has 5-min intervals, and the other is the final product produced after 4 weeks, which is at 2-hour intervals. The estimated ZTD values for the common epochs using the new strategy were compared with both the IGS near-real-time (NRT) and the IGS final ZTD (Final) products and summarised in Table 9.

Atmos. Meas. Tech. Discuss., https://doi.org/10.5194/amt-2017-321
Manuscript under review for journal Atmos. Meas. Tech.
Discussion started: 10 November 2017

Table 9 RMS of the daily difference of PPP solutions from the IGS weekly solutions for 12 weeks for all stations

Tropospheric Delay Method	ZTD reference value	Daily difference (RMS) (mm)				Tropospheric difference (mm)		
		Orbits & Clocks	E	N	U	Mean	STD	RMS
The New strategy	NRT	NRCan	4.0	3.8	10.0	1.1	5.8	5.9
	Final	NRCan				2.0	5.8	6.1
	NRT	IGS_final	7.9	4.5	18.7	1.1	5.8	5.7
	Final	IGS_final				2.0	5.9	5.5

4.5. Global Validation using Real-Time Products

The new strategy was evaluated in a pseudo *real time* situation; the same IGS data sets as considered previously in Table 8 were used. The PPP processing strategy was the same as before, except it was performed using IGS real-time IGS01 satellite ephemerides and satellite clock offsets. The real-time products were not available for DOY 10, 11, 128–130, 154–158, 191–193, 279–284, 306–312, and 341–345, and therefore these days were excluded. The estimated ZTD from the PPP using the new strategy was compared with the final and near-real-time ZTDs.

Table 10 RMS of the daily difference of PPP solutions from the IGS weekly solutions using real-time products

Tropospheric Delay Method	ZTD reference Value	Orbits & Clocks	Daily difference (RMS) (mm)			Tropospheric difference (mm)		
			E	N	U	Mean	STD	RMS
The New strategy	NRT	IGS real-time	20.3	15.7	27.7	1.3	8.0	8.1
	Final					2.0	7.8	8.1

Atmos. Meas. Tech. Discuss., https://doi.org/10.5194/amt-2017-321
Manuscript under review for journal Atmos. Meas. Tech.
Discussion started: 10 November 2017

It is important to highlight that these results compare the final IGS ZTD values to those based on real-time PPP. This validation clearly shows that the real-time results are almost as good as the post-processed final results mentioned in Table 8, and therefore that the new strategy may be used for PPP in real time when users have access to the real-time products, without the need to implement a tropospheric model except for mapping functions.

5. Results Discussion of The Two Methods

It is important to explain why the tropospheric models do not have the ability to produce accurate ZTDs, but do have a consistent level of accuracy among them. Zhang and Gao (2001) mentioned that the consistency of the position vector could reflect the quality of the troposphere delay estimates. However, the results in Tables 5 and 6 show this is not necessarily true for the quality of the tropospheric delay in the PPP case. At this level of accuracy, the position vector can be estimated precisely while the estimated troposphere will not be estimated precisely because the receiver clock offset and the estimated ambiguities absorb some of the error in the tropospheric delay estimation, so the coordinates are not affected.

Considering the results in Table 5, when using a model for the hydrostatic component and estimating the wet delay, the receiver clock will absorb some of the effect of uncertainty in the modelled hydrostatic component. This is evident in Figure 5, which illustrates the differences between the estimated carrier receiver clock from PPP GPS and the estimated carrier receiver clock from PPP GPS using the new strategy for three sample stations in the UK: DRUM (Drumalbin), FARB (Farnborough), and KEYW (Keyworth) for DOY 12 (12/01), 2014.

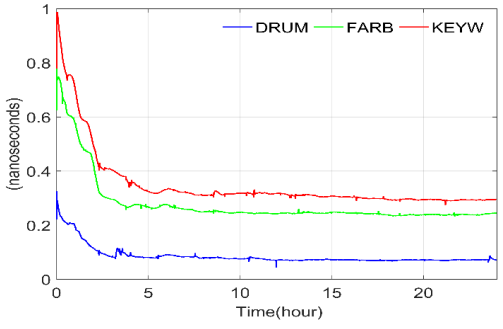

Fig. 5 Differences between the estimated carrier receiver clock from the new strategy and the carrier receiver clock from the traditional method

Atmos. Meas. Tech. Discuss., https://doi.org/10.5194/amt-2017-321
Manuscript under review for journal Atmos. Meas. Tech.
Discussion started: 10 November 2017

Atmospheric Measurement Techniques Discussions

Figure 6 shows an example of phase residuals, the estimated ionosphere-free ambiguity and the widelane ambiguity for satellite PRN 11, DRUM station using the tropospheric model for the hydrostatic component with an estimation of the wet component (left) and using the new strategy (right) for tropospheric estimation, respectively. It can be seen that there is neither an effect on the phase residual nor the widelane ambiguity.

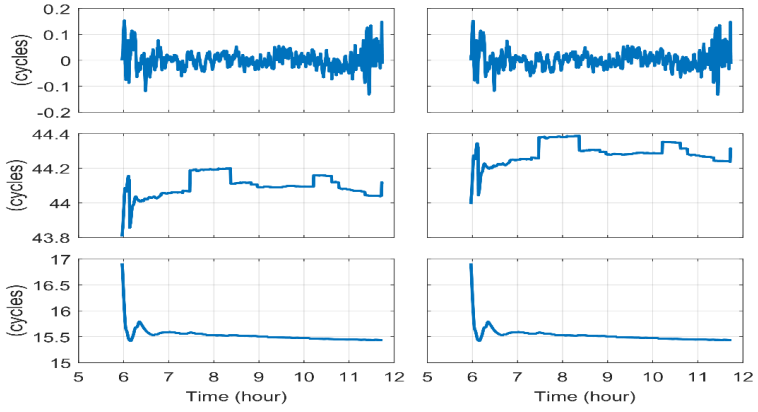

Fig. 6 Tropospheric model effect on phase residuals (top), ionospheric-free-ambiguity (middle) and the widelane ambiguity (bottom) using a model for the hydrostatic component with an estimation for the wet component (left); using the new strategy for phase residual, ionospheric ambiguity and widelane ambiguity (right).

It can be concluded from this that the unmodeled tropospheric delay and the receiver clock, as well as the ionosphere-free ambiguity, are linked to each other. In PPP applications that require ambiguity fixing, an error in the ionosphere-free ambiguity, caused by unmodeled tropospheric delay, will result in incorrect narrow lane ambiguities and hence an incorrect position solution. This is because the narrow lane ambiguities are computed from the non-integer ionosphere-free ambiguities and the integer-valued widelane ambiguities.

Atmos. Meas. Tech. Discuss., https://doi.org/10.5194/amt-2017-321
Manuscript under review for journal Atmos. Meas. Tech.
Discussion started: 10 November 2017

Atmospheric Measurement Techniques Discussions

6. PPP Improvement When using the Alternative Tropospheric Strategy

The suitability of the alternative strategy for tropospheric ZTD estimation can also be reflected in the PPP performance in terms of the convergence time and repeatability as follows.

6.1. Convergence time

The efficiency of the new strategy for tropospheric estimation is also reflected in the PPP performance. It is known that the convergence time for the PPP solution is longer for the height component and this has a relation with the tropospheric estimation. Applying the new strategy not only gives high accuracy ZTD from the PPP solution but it also improves the convergence time. The convergence time was defined as the required time from the first epoch to reach to a chosen agreement with the '*truth values'* from the DD solution. A significant improvement can be seen in Figure 7, where the coordinate convergence time is shown for 20, 10, and 5 cm for the height component for all models and all PPP cases, using the dataset in Table 4. The improvement in the time taken to converge to 5 cm, compared to the current strategy, using UNB3m, GPT, Saastamoinen, and SBAS models were 49, 66, 44 and 43 minutes for PPP GPS (top), 31, 53, 30 and 29 minutes for PPP GLO (middle), and 28, 37, 22 and 23 minutes for PPP GPS+GLO (bottom), respectively.

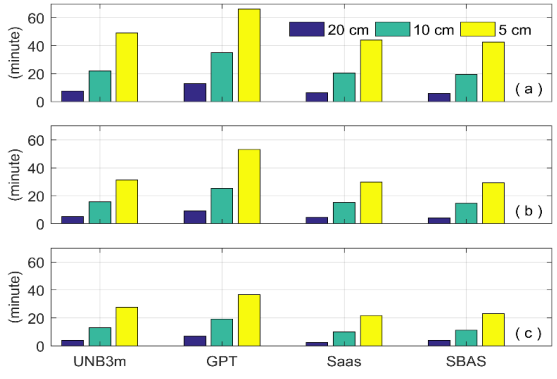

Fig. 7 Improvements in the convergence time when using the new strategy for PPP GPS (top), PPP GLO (middle) and PPP GPS+GLO (bottom)

Atmos. Meas. Tech. Discuss., https://doi.org/10.5194/amt-2017-321
Manuscript under review for journal Atmos. Meas. Tech.
Discussion started: 10 November 2017

Atmospheric Measurement Techniques Discussions

6.2. The Improvement on one-year Repeatability

Another potential improvement is in the repeatability over a long period. This can be seen in Figure 8, which represents a comparison of two OSGB stations ALDB and AMER using the conventional and alternative tropospheric strategies.

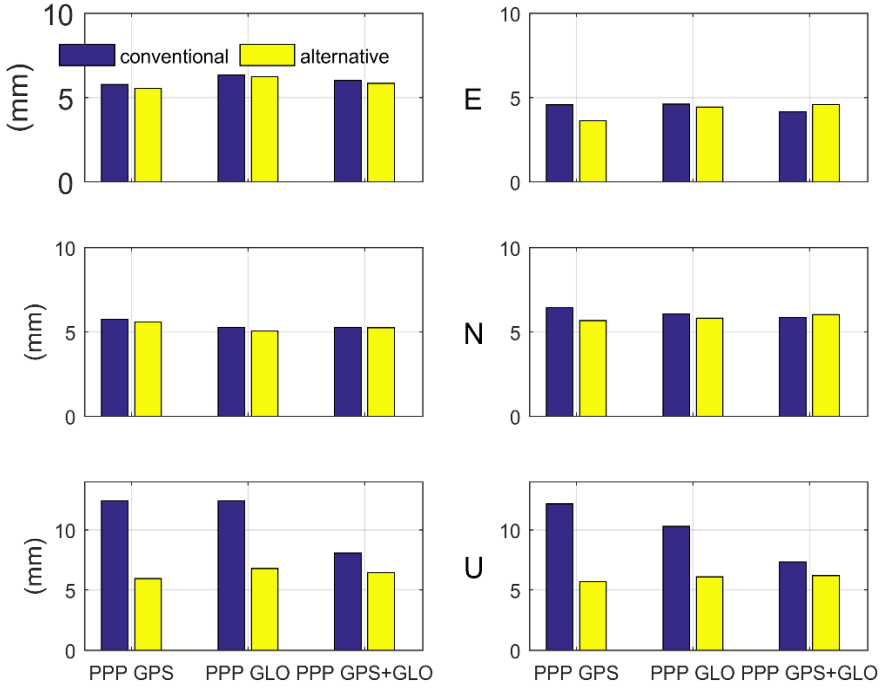

Fig. 8 Comparison between the repeatability analysis when using a model for troposphere and by using the alternative tropospheric strategy (AMER Left, ALDB Right)

From Figure 8, it can be seen that the main improvement obtained is in the repeatability of the station coordinate Up component to be 51.9% (GPS), 45.4% (GLO) and 20.0% (GPS+GLO) for AMER station, 53.2% (GPS), 40.5% (GLO) 15.4% (GPS+GLO) for ALDB station.

7. Conclusions

This study set out to compare the effect of different models for the hydrostatic component and to present an alternative method to improve the estimation of ZTD from PPP with post processing and with *real- time* estimation, without using any external tropospheric information.

Based on the tropospheric analysis, it can be concluded that the traditional method for estimating ZTD does not have the ability to produce millimeters accuracy of tropospheric delay, even though the position estimation is accurate, because the receiver clock absorbs the unmodeled tropospheric delay and the estimated ambiguity.

The presented method does not rely on any zenith tropospheric delay models for the hydrostatic component. Instead, it separates the hydrostatic and the wet components using different mapping functions and different process noise in an extended Kalman filter. Following this method, the estimated ZTD_{ppp} can be modelled more accurately and within millimeters accuracy compared to the ZTD_{DD}. A series of validations were conducted for the alternative tropospheric strategy using PPP GPS, PPP GLO and PPP GPS+GLO. Validation using 7 consecutive days were first performed, followed by an expanded regional validation that was done for a seven week dataset of OSGB stations in the UK, and then a long-term (over one year) validation for 22 OSGB stations. A global validation using ~76 stations IGS stations was then done over a different period, and conducted in three stages, using EMX final, IGS final and IGS real-time precise products. The estimated tropospheric ZTD compared favorably with the IGS final and near real-time solutions. It was also proposed that this approach can be used in *real-time* as well as in post-processing without a significant difference between the results.

Lastly, it was shown that with the alternative tropospheric strategy, PPP users will not only obtain an accurate tropospheric ZTD, but they will also have an improvement in the convergence time and the repeatability of station height over the long term.

Acknowledgment: The first author acknowledges the financial support he received from his government in Iraq during the period of his postgraduate research study at the University of Nottingham.

References

BOEHM, J., HEINKELMANN, R. & SCHUH, H. 2007. Short Note: A global model of pressure and temperature for geodetic applications. *Journal of Geodesy,* 81**,** 679-683, DOI: 10.1007/s00190-007-0135-3.

BÖHM, J., MÖLLER, G., SCHINDELEGGER, M., et al. 2014. Development of an improved empirical model for slant delays in the troposphere (GPT2w). *GPS Solutions*, 19**,** 433-441, DOI: 10.1007/s10291-014-0403-7.

CHEN, G. & HERRING, T. A. 1997. Effects of atmospheric azimuthal asymmetry on the analysis of space geodetic data. *Journal of Geophysical Research-Solid Earth*, 102**,** 20489-20502, DOI: 10.1029/97jb01739.

CHEN, W. R., GAO, C. F. & PAN, S. G. 2014. Assessment of GPT2 Empirical Troposphere Model and Application Analysis in Precise Point Positioning. *China Satellite Navigation Conference (CSNC) 2014 Proceedings: Volume II.*

COLLINS, P., BISNATH, S., LAHAYE, F., et al. 2010. Undifferenced GPS Ambiguity Resolution Using the Decoupled Clock Model and Ambiguity Datum Fixing. *Navigation*, 57**,** 123-135, DOI: 10.1002/j.2161-4296.2010.tb01772.x.

DACH, R., BROCKMANN, E., SCHAER, S., et al. 2009. GNSS processing at CODE: status report. *Journal of Geodesy*, 83**,** 353-365, DOI 10.1007/s00190-008-0281-2.

DACH, R., HUGENTOBLER, U., FRIDEZ, P., et al. 2007. Bernese GPS software version 5.0 (user manual of the Bernese GPS software version 5.0). *AIUB—Astronomical Institute, University of Bern, Switzerland.*

DEE, D. P., UPPALA, S. M., SIMMONS, A. J., et al. 2011. The ERA-Interim reanalysis: configuration and performance of the data assimilation system. *Quarterly Journal of the Royal Meteorological Society*, 137**,** 553-597, DOI: 10.1002/qj.828.

DODSON, A. H., BINGLEY, R. M., PENNA, N. T., et al. 2000. A national network of continuously operating GPS receivers for the UK. *Geodesy Beyond 2000.*

DOW, J. M., NEILAN, R. E. & RIZOS, C. 2009. The International GNSS Service in a changing landscape of Global Navigation Satellite Systems. *Journal of Geodesy*, 83**,** 191-198, 10.1007/s00190-008-0300-3.

FENG, S., OCHIENG, W., MOORE, T., et al. 2008. Carrier phase-based integrity monitoring for high-accuracy positioning. *GPS Solutions,* 13**,** 13-22, DOI: 10.1007/s10291-008-0093-0.

KOUBA, J. 2009. *A guide to using International GNSS Service (IGS) products* [Online]. ftp://ftp.igs.org/pub/resource/pubs/UsingIGSProductsVer21.pdf. Available: ftp://ftp.igs.org/pub/resource/pubs/UsingIGSProductsVer21.pdf [Accessed].

KRUEGER, E., SCHUELER, T. & ARBESSER-RASTBURG, B. 2005. The standard tropospheric correction model for the European satellite navigation system Galileo. *XXVIIIth General Assembly of the International Union of Radio Science (URSI).* New Delhi, India.

LAGLER, K., SCHINDELEGGER, M., BOHM, J., et al. 2013. GPT2: Empirical slant delay model for radio space geodetic techniques. *Geophysical Research Letters,* 40**,** 1069-1073, DOI: 10.1002/grl.50288.

LEANDRO, R., SANTOS, M. & LANGLEY, R. B. UNB Neutral Atmosphere Models: Development and Performance. Proceedings of the 2006 National Technical Meeting of The Institute of Navigation, 18-20 January 2006 Monterey, CA. 564-73.

LI, W., YUAN, Y. B., OU, J. K., et al. 2012. A new global zenith tropospheric delay model IGGtrop for GNSS applications. *Chinese Science Bulletin,* 57**,** 2132-2139, DOI: 10.1007/s11434-012-5010-9.

LIU, Z. Z. 2011. A new automated cycle slip detection and repair method for a single dual-frequency GPS receiver. *Journal of Geodesy,* 85**,** 171-183, DOI: 10.1007/s00190-010-0426-y.

MCCARTHY, D. D. & PETIT, G. 2004. IERS conventions (2003). Germany: DTIC Document.

MEINDL, M., SCHAER, S., HUGENTOBLER, U., et al. 2004. Tropospheric gradient estimation at CODE: Results from global solutions. *Journal of the Meteorological Society of Japan,* 82**,** 331-338, DOI: 10.2151/jmsj.2004.331.

NIELL, A. E. 1996. Global mapping functions for the atmosphere delay at radio wavelengths. *Journal of Geophysical Research-Solid Earth,* 101**,** 3227-3246, DOI: 10.1029/95jb03048.

PACE, B., PACIONE, R., SCIARRETTA, C., et al. 2010. Estimating Zenith Total Delay Residual Fields by using Ground-Based GPS network. *Proceedings of XX EUREF Symposium.* Gävle, Sweden.

PANY, A., WRESNIK, J., BÖHM, J., et al. 2007. Optimum modeling of troposphere and clock parameters in VLBI. *Proceedings of the 18th European VLBI for Geodesy and Astrometry Working Meeting.* Vienna.

PENNA, N., DODSON, A. & CHEN, W. 2001. Assessment of EGNOS tropospheric correction model. *Journal of Navigation,* 54**,** 37-55, DOI: 10.1017/S0373463300001107.

RTCA 1996. *Minimum Operational Performance Standards for Global Positioning System/Wide Area Augmentation System Airborne Equipment: Hauptbd,* RTCA.

SAASTAMOINEN, J. 1972. Atmospheric correction for the troposphere and stratosphere in radio ranging satellites. *The Use of Artificial Satellites for Geodesy.* Washington, D. C: American Geophysical Union.

SAASTAMOINEN, J. 1973. Contributions to the theory of atmospheric refraction. *Bulletin Géodésique,* 107**,** 13-34, DOI: 10.1007/bf02522083.

SCHUELER, T., HEIN, G. W. & EISSFELLER, B. 2000. Improved Tropospheric Delay Modeling Using an Integrated Approach of Numerical Weather Models and GPS. *Proceedings of the 13th International Technical Meeting of the Satellite Division of The Institute of Navigation (ION GPS 2000).* Salt Lake City, UT.

WU, J., WU, S., HAJJ, G., et al. 1993. Effects of antenna orientation on GPS carrier phase. *Manuscripta Geodaetica,* 18**,** 91-98,

YANG, L., HILL, C. & MOORE, T. 2013. Numerical weather modeling-based slant tropospheric delay estimation and its enhancement by GNSS data. *Geo-spatial Information Science,* 16**,** 186-200, DOI: 10.1080/10095020.2013.817107.

ZHANG, Y. & GAO, Y. 2001. Influence Analysis of Tropospheric Model and Mapping Function on Precise Tropospheric Delay Estimation Using PPP. *Proceedings of the 19th International Technical Meeting of the Satellite Division of The Institute of Navigation (ION GNSS 2006).* Fort Worth, TX.

ZUMBERGE, J. F., HEFLIN, M. B., JEFFERSON, D. C., et al. 1997. Precise point positioning for the efficient and robust analysis of GPS data from large networks. *Journal of Geophysical Research-Solid Earth,* 102**,** 5005-5017, DOI: 10.1029/96jb03860.